Pramāṇa – J. Phys., Vol. 27, No. 6, December 1986, pp. 821–833. © Printed in India.

XANES and EXAFS study of some metal-metalloid glasses

K B GARG, KAVITA S JERATH, H S CHAUHAN and USHA CHANDRA

Department of Physics, University of Rajasthan, Jaipur 302004, India

MS received 14 July 1986; revised 24 September 1986

Abstract. XANES and EXAFS techniques are proving very popular in the study of local environment in disordered systems. Results of such studies in a large number of metal (Fe, Co, Ni, etc)-metalloid (B, Si, C, etc) glasses are reported. Experiments were done with synchrotron radiation† as well as an x-ray tube. The values of bond lengths and co-ordination numbers computed from one-electron single scattering Fourier transform method turn out substantially smaller. The values of bondlength determined from the other EXAFS calculation method and the multiple-scattering computation scheme show good agreement. Importance of choice of suitable reference materials for analysis of data is emphasized.

Keywords. XANES; phase-shifts; metallic-glasses; co-ordination number; bond distances; near-neighbour environment; single-scattering; multiple-scattering; polk model; synchrotron radiation.

PACS No. 78·70D

1. Introduction

Metallic glasses are metastable alloys with high electrical and thermal conductivities, better known for their very low magnetic coercivity, high mechanical strength, ductility in bending and corrosion resistance. The properties depend much on their composition. The most important class of these amorphous metallic glasses is the transition metal-metalloid (T-M) glasses. The (T-M) glasses typically contain about 80 at. % Fe, Co or Ni with the remainder being B, C, Si, P, or Al. The presence of the metalloids is necessary to lower the melting point making it possible to quench the alloy through its glass temperature rapidly enough to form the amorphous phase. Once made, the same metalloids stabilize the amorphous phase.

Study of structure and bonding in metallic glasses is of considerable interest and several techniques have been employed for it, namely x-ray scattering (Chen *et al* 1982), neutron scattering (Nold *et al* 1981), electron scattering (Paasche *et al* 1982) and Mössbauer spectroscopy (Dubois and Caer 1982) etc. Of late, extended x-ray absorption fine structure (EXAFS) and x-ray absorption near edge structure (XANES) methods have become increasingly important, ostensibly because they are simpler and can probe the local environment around each species in a multi-component system (Raoux *et al* 1983). XANES measures the local density of unoccupied states of a particular symmetry and a direct comparison of the absorption edges of the metal in

† The experimental work was done at EXAFS 5·1 Station at Daresbury Laboratory, U.K.

elemental and amorphous state can give useful information on the electronic changes experienced by the atoms in the amorphous state (Crescenzi *et al* 1980). With recent major advances in the theory it is now possible to do multiple-scattering calculations on XANES and show how sensitive XANES calculations are to changes in the local symmetry (Gaskell *et al* 1982). It is thus likely that these multiple scattering XANES calculations may, in the near future, yield valuable information on triplet or even higher order correlations while all other techniques are only sensitive to pair correlation functions (Raoux *et al* 1983). In an EXAFS experiment, the quantity of interest is the modulation $\chi(k)$ of the x-ray absorption coefficient $\mu(h\nu)$ at energies above the absorption edge. It extends to several hundreds of electron volts above the edge and is ascribed to local interference effects of spherical waves emerging from the absorbing atom, representing the outgoing photoejected core electron, with the spherical waves backscattered by the neighbouring atoms (Sayers *et al* 1970). The EXAFS interpretation, therefore, yields the near-neighbour distances and the co-ordination numbers. Further, since the energy dependence of the backscattered amplitude changes with the atomic number of the scatterer, it is also possible to identify the scattering species (Hayes *et al* 1978).

The major interest in the EXAFS study of metallic glasses centres around the question whether or not the glass structure exhibits a chemical ordering and, if it does, how can the EXAFS yield to new structural insight. The structure of such T-M glasses has been postulated by Polk (1970) to comprise of a dense-random-packing of hard spheres (DRPHS). Dense-random-packed structures for these glasses allow the non-metallic atom to occupy poly-hedral cavities of several different types, only one of which resembles the local coordination observed in the crystalline state. The metalloid atoms, it is concluded, would sit in eightfold—or ninefold—co-ordination with the metal atom in the T-M alloys at the atomic ratio [T]:[M] of 80:20. Polk's model further postulates metalloid-metalloid avoidance and a metal-metal near-neighbour distance smaller than the sum of the atomic radii of the constituent atoms. Earlier EXAFS (Chen *et al* 1982) results for $T_{80}M_{20}$-type glasses have generally substantiated the Polk model, but serious quantitative differences have been reported later (Chen *et al* 1982; Wong 1981; Lamparter *et al* 1982; Haensel *et al* 1980; Eisenberger and Brown 1979).

In this paper we report the XANES and EXAFS results on a number of T(Fe, Co, Ni, Mo)- M(B, Si, C) glasses and discuss the changes in electronic structure and bond length. The erroneous results obtained in calculation of co-ordination numbers are discussed to highlight the shortcomings of the EXAFS method when applied to T-M glasses. Bond lengths are also estimated from the graphic analysis method (Lytle *et al* 1975) of the EXAFS theory and the new multiple scattering formalism (Bianconi *et al* 1983) for the XANES calculation.

2. Experimental

Metglas ribbons of thickness $\sim 25\ \mu m$ were supplied by Allied Chemicals and Goodfellow Metals. These were thinned by polishing upto the optimal thickness ($\sim 10\ \mu m$), thus minimizing the spurious effects induced by harmonics (Goulon *et al* 1982). Calibration was done using pure metal foils $\sim 8\ \mu m$ thick. The XANES and EXAFS measurements were performed at the K-edges of iron, cobalt and nickel at the

EXAFS-5·1 station at Daresbury (U.K.) using the synchrotron radiation source operating at 1·8 GeV; 200 mA in the multi-bunch mode and a Si(220) channel-cut monochromator. For analysis of the EXAFS data by Fourier-transform method the EXCALIB, EXBACK and EXCURVE programs (Gurnam *et al* 1984) were employed. The last one is used to calculate theoretical spectra from a one-electron single-scattering model employing a rapid curved-wave computational scheme. The spectra were recorded at ~ 300° K with a statistics of better than 0·2% at the peak.

3. Results and discussion

The spectra recorded after calibration and normalization are shown in figures 1–3. Figure 1 shows the iron K-spectra in Fe metal and five metallic glasses with their Fe content varying from 40 to 81%. Figure 2 shows the cobalt K-spectra of two glasses as well as the metal whereas figure 3 shows the nickel K-spectra in two glasses and the metal. As can be seen from these figures, the metal spectrum in each case displays much

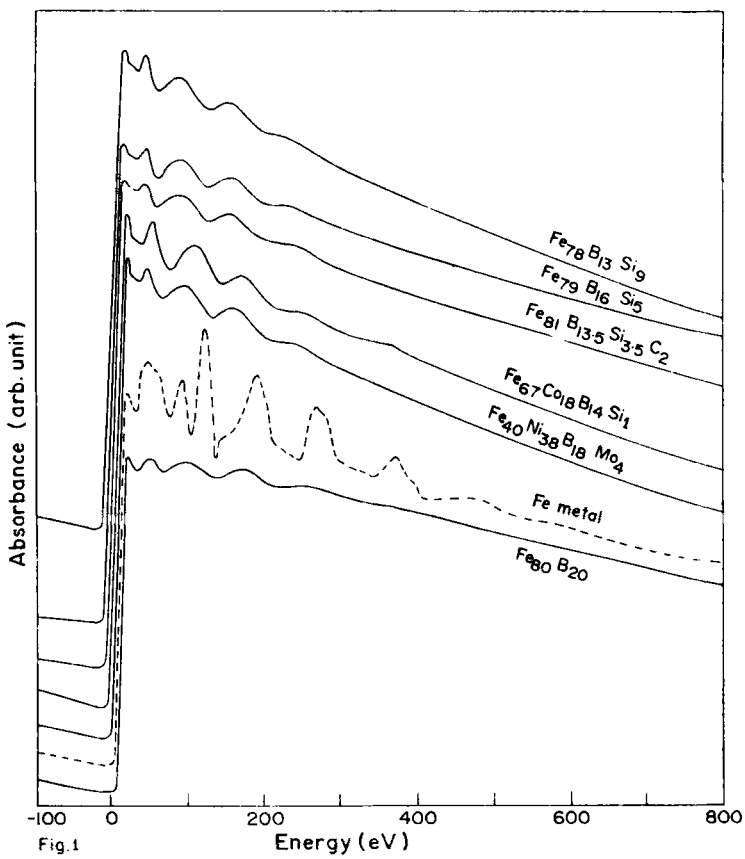

Figure 1. Iron K-absorption spectra—XANES and EXAFS—in Fe-B glasses (line) and metal (dashed). The edge in glasses shifts to lower energies and its main peak also loses in intensity.

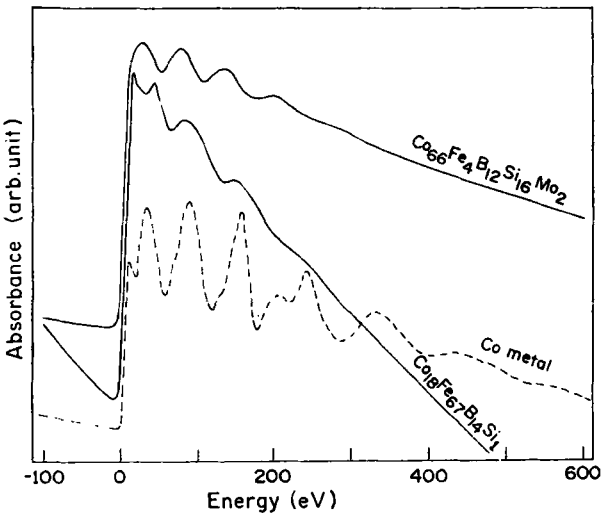

Figure 2. Co K-absorption spectra in metal (dashed) and Co, Fe-B glasses (line).

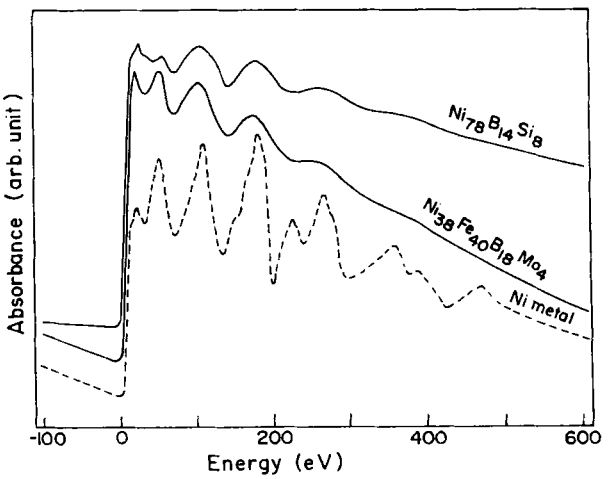

Figure 3. Ni K-absorption spectra in metal (dashed) and Ni-B and Ni, Fe-B glasses (line).

more fine structure in its XANES and EXAFS regions as compared to the spectra of corresponding glasses. Confining first our attention to the spectra in the EXAFS region ($\sim$ 40 eV above the absorption edge), these appear to possess a sinewave form indicating how the first near-neighbour shell dominates in back-scattering of the photo-electron wave due ostensibly to the amorphous nature of these samples. The EXAFS spectra of the metals, on the other hand, have contributions coming from a number of near-neighbour shells due to their high crystalline symmetry and consequently show much fine structure. Also, Fe, Co and Ni spectra in the various glasses all appear remarkably similar to one another, further emphasizing the essential similarity of the near-neighbour environment around them. Even the interpeak separations in the EXAFS region are virtually the same in not only the spectra of the

same metal but also in those of different metals. There is, however, one exception—$Co_{66}Si_{16}B_{12}Fe_4Mo_2$ (figure 2) while having a similar EXAFS spectrum shows some dramatic variation in its XANES part.

3.1 *EXAFS data*

The EXAFS technique which employs one-electron single-scattering computational scheme is firmly established as a powerful method for study of near-neighbour environment.

The EXAFS spectra are explained by treating the ejected photo-electron as a spherical wave expanding in the lattice and getting partially scattered by neighbouring atoms which may be treated as point scatterers. The total scattered wave is determined from superposition of the waves scattered by each atom and the EXAFS determined from the dipole transition matrix between initial and the final photo-electron states.

In the single-scattering computation scheme (Wong and Liebermann 1984 and Cargrill III 1984) hereafter referred to as the FT (Fourier transform) method, the EXAFS function $\chi(k)$ is given by

$$\chi(k) = \sum_j \frac{N_j}{Kr_j^2} \exp(-2k^2\sigma_j^2) F_j(k) D_j(k) \sin[2kr + \phi_j(k)], \tag{1}$$

where F_j is the backscattering amplitude from each of the N_j neighbouring atoms of type j, and $\phi_j(k)$ is the total phase-shift experienced by the photo-electron, including central atom and backscattered contributions. σ_j is the mean square width of a gaussian distribution of atoms of type j in a shell of average radius r_j about the absorbing atom. The factor $D_j \leqslant 1$ takes into account losses due to multielectron excitations and inelastic scattering. This is sometimes represented in terms of a K-dependent mean free path $\lambda(k) = \tau/k$ with $D_j(k) = \exp[-2r_j/\lambda(k)]$.

A more general expression for $\chi(k)$ can be written using partial distribution function $\rho_{ij}(r)$,

$$\chi(k) = \sum_j \int \frac{4\pi r^2 \rho_{ij}}{kr^2}(\gamma) F_j(k) D(r, k) \sin[2kr + \phi_j(k)] \, dr, \tag{2}$$

where the sum is over different chemical elements j in the alloy for absorption by element i. Only nearby atoms contribute to the integral because of the limited photo-electron mean free path included in $D(r, k)$.

The Fourier transform of $\chi(k)$

$$\phi_n(r) = \frac{1}{\sqrt{2\pi}} \int_{k_{min}}^{k_{max}} k^n \chi(k) \exp(2ikr) \, dk \tag{3}$$

is a radial structure function having both real and imaginary parts. Various choices of exponent $n = 0, 1, 2, 3$ and of integration limits, k_{min} and k_{max}, are used in transforming experimentally determined $\chi(\cdot)$ functions. Frequently occurring distances r_j (see equation (1)) and sharp maxima in ρ_{ij} (see equation (2)) give rise to maxima in $|\phi_n(r)|$. For a well-separated maxima in $|\phi_n(r)|$ Fourier transformation can be used to obtain the corresponding components of $\chi(k)$.

Amorphous systems like metallic glasses offer a very attractive opportunity for use of the EXAFS technique. Experience has, however, shown that some serious limitations

may arise when the technique is applied to amorphous systems like metallic glasses. One of the perennial problems in these materials is the possible existence of a non-gaussian pair distribution for which one may have to use an asymmetry factor in the distribution function (Haensel *et al* 1980). There is, however, no way of logically determining the value of such an asymmetry parameter. The other problem arises from a possible absence of crystalline compounds of known structure having composition identical to the glasses. Absence of such a suitable reference material makes it difficult to generate self-consistent phase-shifts and backscattering amplitude functions which, in turn, may lead to errors in evaluating of bond distances and co-ordination numbers in amorphous phase (Wong and Liebermann 1984). The Fe–B glasses are particularly stricken with this problem. Fe_2B is the crystalline phase nearest in composition to the $Fe_{80}B_{20}$ glasses and hence is not reliable enough for calculation of the phase-shifts.

Our own results on metallic glasses serve to highlight some of these facts. As pointed out earlier, the EXAFS spectra look alike in all the glasses studied by us, emphasizing the fact that the near-neighbour environment does not undergo any big changes with changes in composition and type of metalloid and other metal atoms present in the system. Table 1 incorporates our data on the results of our measurement on the iron K-absorption edge in a number of glasses. As usual, after subtracting the background, deglitching, marking off the Fermi level and normalizing the spectrum we chopped off the XANES part extending upto about 50 eV for EXAFS analysis. The post-edge background was then subtracted defining a polynomial of upto order four and the EXAFS signal $\chi(k)$ extracted from the spectrum. The FT of $\chi(k)$ yielded a broad radial peak around 2·4 Å which is a little asymmetric on the low R side. Theoretical calculations in the single-scattering approximation were made on basis of (1) and (2). Of the various parameters on the right side of these equations the scattering parameter phase-shift $\phi_j(k)$ was calculated for fcc Fe assuming muffin-tin potential. These phase-shifts were tested on the EXAFS spectrum of Fe metal and the results are shown in figure 4 and table 2. The calculated and observed $\chi(k)$ and FT for the first six shells show a very good agreement. In fact, the calculated phase-shifts were first refined using Daresbury ITPR program to yield best fits for the Fe EXAFS in metal. The program was then allowed to iterate on the threshold E_F, the bond distance R_j, co-ordination

Table 1. Values of bond lengths (in Å) in Fe-B glasses as calculated from the EXAFS (FT), EXAFS (GA) and XANES measurements.

	EXAFS				
	F.T. method		Graphic analysis		
Sample	Coordination No.	R	method ($\alpha = 1{\cdot}60$)	XANES ($\bar{V} = -230{\cdot}8$)	Reference
$Fe_{40}Ni_{38}B_{18}Mo_4$	—	—	2·57	2·58	—
$Fe_{67}Co_{18}B_{14}Si_1$	—	—	2·57	2·58	—
$Fe_{78}B_{13}Si_9$	3·1	2·40	2·61	2·58	—
$Fe_{79}B_{16}Si_5$	3·3	2·39	2·57	2·58	—
$Fe_{80}B_{20}$	4·5	2·41	2·58	2·58	2·58 (Defrain *et al* 1984) 2·46 (Haensel *et al* 1980) 2·30 (Crescenzi *et al* 1981)
$Fe_{81}B_{13.5}Si_{3.5}C_2$	—	—	2·57	—	—

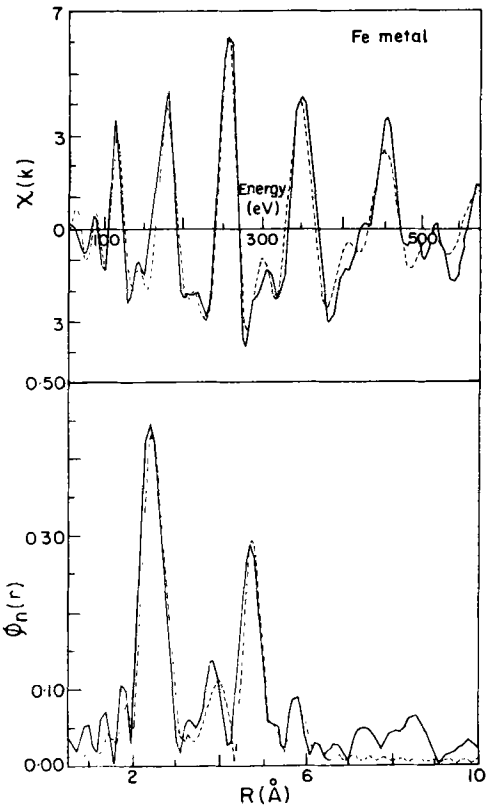

Figure 4. (a) The observed (line) and calculated (dashed) $\chi(k)$ for the K EXAFS spectrum of Fe in metal. Calculations were done for six n-n shells. (b): The observed and calculated Fourier transform for the above.

Table 2. Values of the co-ordination number N and bond length R(Å) for Fe metal obtained from the EXAFS (FT) analysis.

N	R
8·0	2·48
6·0	2·84
12·0	4·07
24·0	4·78
8·0	5·07
6·0	5·91

number N_j and the Debye-Waller factor σ_j in order to get the best fits for the metallic glass EXAFS. The dashed curves in figures 5 and 6 serve to illustrate these fits in three of the samples. The fits for both $\chi(k)$ as well as the FT appear to be very good and yet the values of co-ordination number achieved for the first shell are very low in comparison

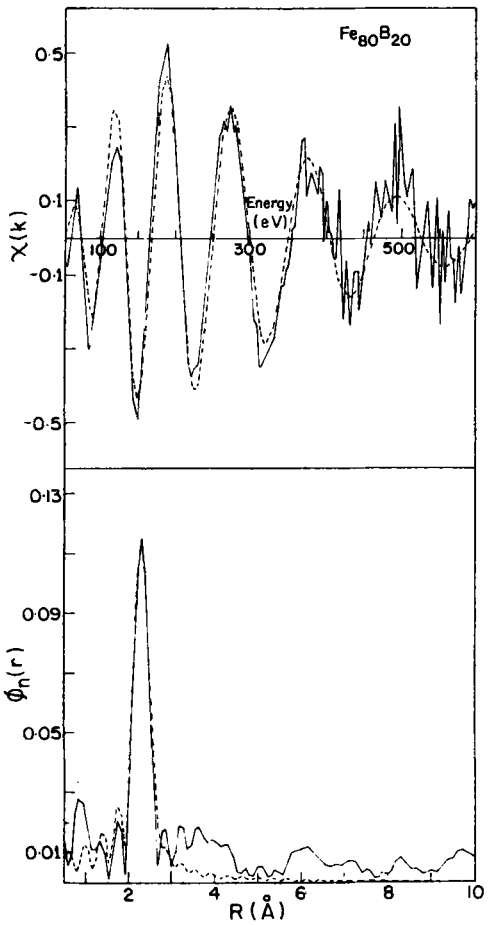

Figure 5. (a) The observed (line) and calculated (dashed) $\chi(k)$ for the K EXAFS spectrum of $Fe_{80}B_{20}$. Calculations were done for the first two n-n shells (b) The observed and calculated Fourier transform for the above.

to the data available from other techniques. Instead of a co-ordination number around 10 the values obtained by us (table 1) hinge around 3. The presence of asymmetric pair distribution and absence of suitable reference material for calculation of phase-shifts are perhaps both responsible for this discrepancy in our data. Haensel *et al* (1980) have been able to achieve a better agreement for Fe-B glasses employing an asymmetry parameter of 0·17 in their data analysis. In Ni-B glasses, on the other hand, Wong and Liebermann (1984) have been able to achieve agreement by preparing glass samples of composition identical to the crystalline Ni_2B. Such puzzling discrepancies from EXAFS data are well known (Raoux *et al* 1983) in metallic glasses. As expected, the values of bond length as well as co-ordination number so determined turn out to be appreciably smaller than those determined by others after suitable corrections. A comparison of the bond length values mentioned in table 1 serves to highlight this point.

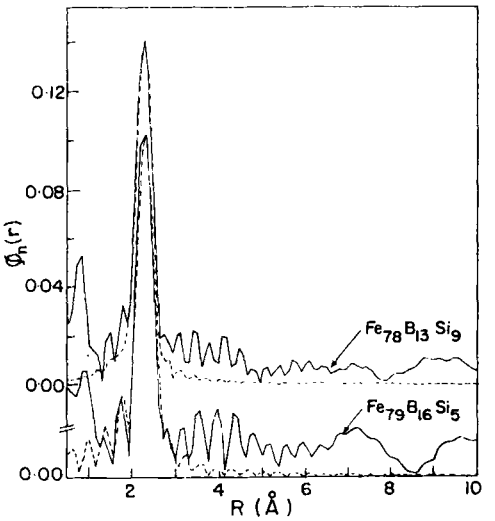

Figure 6. Observed (continuous) and calculated (dashed) Fourier transforms for the EXAFS spectra for $Fe_{78}B_{13}Si_9$ and $Fe_{79}B_{16}Si_5$. Calculations done only for the first *n-n* shell.

Since the foregoing FT method in its harmonic approximation does not yield reliable values even of bond distances, we decided to check these against calculations from the EXAFS graphic analysis (GA) method (Lytle *et al* 1975) which is quite adequate for amorphous materials since the back-scattering in these cases is dominated by the first near-neighbour shell. The analysis depends on the argument of $\sin [2kr - \phi_j(k)]$ in (1). Following the treatment by Lytle *et al* (1975), a plot of n vs k where $n = 0, 2, 4$ for the EXAFS maxima and $n = 1, 3, 5$ for minima and k is the corresponding wave vector given by $(0{\cdot}263)^{1/2}$ their energy. Figure 7 gives these plots for the samples studied by us. The slope m of n vs k line is then related to bond length (Lokhande and Chetal 1978) by

$$R - \alpha = m\pi/4. \tag{4}$$

α is a constant which has to be evaluated from the spectrum of a reference material. Fe metal and $Fe_{80}B_{20}$ were employed as alternative systems for reference and it was found that the choice of reference material is very important to the final results. In the present case, the bond distances calculated using $Fe_{80}B_{20}$ as reference material turned out to be more consistent and showed better agreement with results of others. Comparing the bond distance in table 1, one can conclude that the calculated values of bond lengths are higher than those obtained from the FT method and agree with those determined by us from the XANES method (described later in this paper) and those reported by others (table 1).

3.2 *XANES data*

Turning our attention now to the XANES spectra of these samples we find the following facts worth a mention:

(i) Except in $Co_{66}Si_{16}B_{12}Fe_4Mo_2$ (figure 2) the XANES spectra in all others look similar. However, unlike in the EXAFS spectra their inter-peak separations in the XANES region are not identical. Also, the XANES in metals displays narrower and

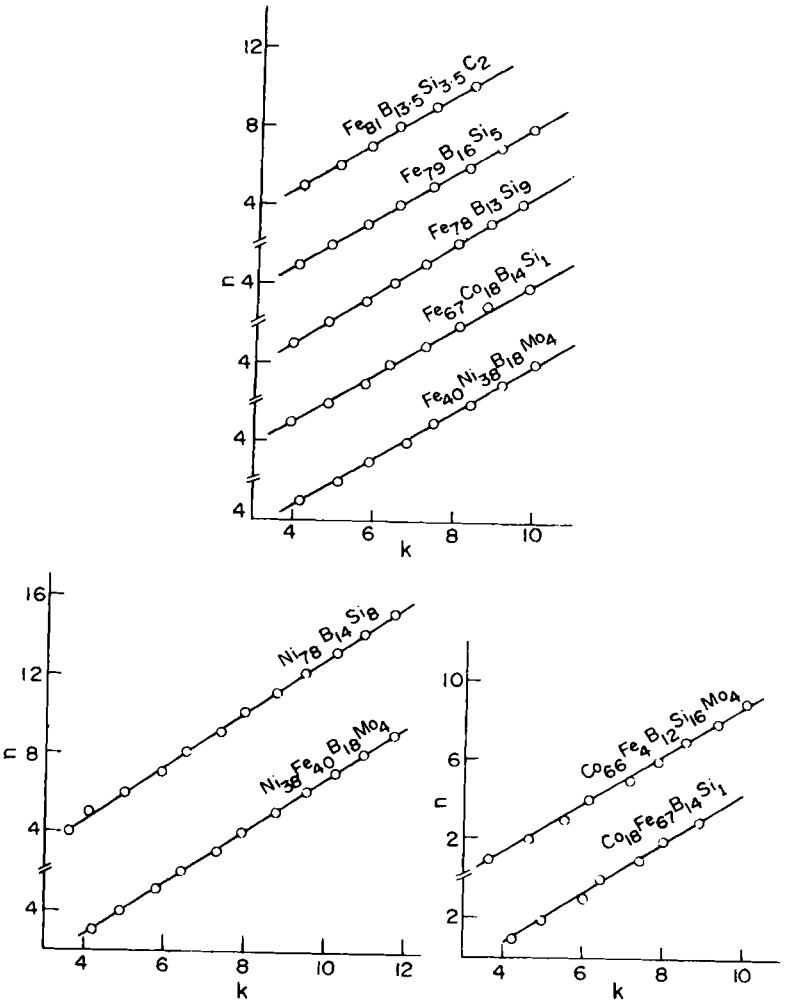

Figure 7. *n* vs *k* plots for the metallic glasses studied.

sharper peaks as compared to the glasses. The recent advent of one-electron multiple-scattering XANES theory (Durham 1983) has shown how the XANES is also strongly dependent on the near-neighbour environment. Using this theory Norman *et al* (Norman *et al* 1985) have recently shown how the extent of fine structure in the XANES spectra in some 3d-oxides depends on the degree of symmetry irrespective of their vastly different bonding and bulk properties. In the present case, the near-neighbour environment in these glasses is described by the DRPHS model (Polk 1970) resulting in greatly reduced symmetry of the corresponding metals. One can thus qualitatively understand the absence of a lot of fine structure in the XANES spectra of these amorphous samples.

(ii) The kink/shoulder observed midway in the absorption edge of metals appears to lose a bit of its prominence in the case of glasses. It is ascribed to the presence of pure 4s states which results in a sudden drop of transition probability. Following this line of

argument the decrease in the prominence of the kink may, therefore, correspond to an increase in hybridization of *s* and *p* symmetric states in these glasses.

(iii) The principal absorption maximum in these glasses also shows a slight decrease in intensity as compared to the case of metal. Amongst other things, addition of metalloid atoms ought to be responsible for this intensity reduction and may be attributed to a charge transfer from metalloid to metal atoms (Raoux *et al* 1983) causing the decrease in the density of empty states of the metal, and a rather strong iono-covalent bonding of the metalloid to its metal neighbours. Detailed calculations (Szmulowicz and Pease 1978) also indicate a *p*-like character for these electronic states just above the Fermi level. This may also be regarded as a significant evidence for dependence of the XANES on changes in electronic structure as well.

We would now like to present our quantitative measurements on these spectra. Table 3 incorporates the results of our measurements on the shift of Fermi level (ΔE_F) in the glasses with respect to that in the metal, the shift of principal absorption maximum (ΔE_A) similarly deduced, the energy of the ejected photo-electron ($E_r = E_A - E_F$) and the values of bondlength, (R) as calculated from the one-electron multiple-scattering formalism (Bianconi *et al* 1983)

$$[E_{r_1} - \bar{V}_1]R_1^2 = [E_{r_2} - \bar{V}_2]R_2^2. \tag{5}$$

The volume average of potential ($\bar{V}$) is calculated using the bond length (R) and photo-electron energy (E_r) values in $Fe_{80}B_{20}$ and $Fe_{79}B_{16}Si_5$ glass in case of Fe-B glasses. In addition to thus ensuring a suitable choice of the reference material, we have, for XANES calculation, employed the bond length values obtained by us for the reference glasses by the GA EXAFS method. The potential when calculated using the E_r and R values of a glass and its corresponding metal yields unsatisfactory values for bond lengths. The bond lengths for Co and Ni glasses have been left out in table 3 for

Table 3. Data on the shift of the edge (ΔE_F) and the principal absorption maximum between metal and glasses, (ΔE_A) photo-electron energy (E_r) and the bond length (R in Å).

Fe metal (eV)	Co metal (eV)	Ni metal		
$E_F = 7111{\cdot}3$	7710·1	8332·1		
$E_A = 7131{\cdot}3$	7725·9	8348·4		
Sample	ΔE_F (eV)	ΔE_A (eV)	$E_r = E_A - E_F$ (eV)	R ($\bar{V} = -230{\cdot}8$)
$Fe_{40}Ni_{38}B_{18}Mo_4$	−0·7	−2·4	19·3	2·58
$Fe_{67}Co_{18}B_{14}Si_1$	−0·7	−1·9	19·4	2·58
$Fe_{78}B_{13}Si_9$	−0·6	−2·7	19·0	2·58
$Fe_{79}B_{16}Si_5$	−0·4	−3·1	19·0	2·58*
$Fe_{80}B_{20}$	+0·2	+1·9	21·7	2·58
$Co_{66}Si_{16}B_{12}Fe_4Mo_2$	−7·4	+1·8	25·0	
$Co_{18}B_{14}Si_1Fe_{67}$	−2·5	−0·08	18·2	
$Ni_{78}B_{14}Si_8$	−0·3	+2·9	19·4	
$Ni_{38}B_{18}Mo_4Fe_{40}$	−0·3	+0·7	17·3	

*Value taken from our EXAFS data; GA method (table 1).

the same reason. Such limitation is quite understandable for the volume averages of potential $\bar{V}_1$ and $\bar{V}_2$ in the above relation can be set equal to each other only in the case of identical bonding and final state. The complex iono-covalent bond in these metallic glasses is evidently quite different from the bond in pure metals. The values of bond length thus calculated are in good agreement with those calculated by us from EXAFS (table 1). Similarly, the values for energy of ejected photo-electron (E_r) are also fairly consistent except in case of $Co_{66}Si_{16}B_{12}Fe_4Mo_2$.

It is also interesting to note from table 3 that all shifts of Fermi level and principal absorption maximum in the Fe-B glasses are negative in each case. No systematic variation can, however, be seen amongst these. The ΔE_F values in Co and Ni glasses are also negative although in the case of the former these are much greater. The shifts can, in general, arise from either charge transfer (Agarwal and Verma 1970) or changes in near-neighbour environment (Garg and Chauhan 1986). Evidently both reasons may hold true in the case of metallic glasses. However, it is difficult to nail it to any one of them. The shift of the principal absorption maximum shows a much different trend and behaviour. In most Co and Ni glasses it is positive resulting thereby in enhanced flatness of the edge. The $Co_{66}Si_{16}B_{12}Fe_4Mo_2$ XANES spectrum presents a vastly different picture in respect of the shifts, the flatness of the edge and the intensity of the principal absorption maximum. Since its EXAFS spectrum is similar to those of other's these differences may primarily be ascribed to the differences in nature of bonding rather than the near-neighbour environment. The presence of other metal atoms viz Fe and Mo in this case may play a significant role in this regard. After all, the role played by the second and third metal atoms in these glasses is far from clearly understood. Of course, that would apply to the $Fe_{40}Ni_{38}B_{18}Mo_4$ and $Fe_{67}Co_{18}B_{14}Si_1$ samples also.

4. Conclusion

To conclude it may be stated that with the recent advent of multiple-scattering XANES theory, the near-neighbour environment in these amorphous glasses can be qualitatively understood in terms of the absence of a lot of fine structure in the XANES spectra. We have also qualitatively explained the local chemistry of these glasses in terms of hybridization, edge shift and charge transfer. Along with this, the values of bond length have been calculated by XANES technique which are in accordance with the values obtained by us from the EXAFS method and also as calculated by other authors. It is important to mention that using the FT method in its harmonic approximation yields much lower values for bond-length and co-ordination number in metallic glasses. For instances, Haensel *et al* (1980) have reported Fe-Fe distance in $Fe_{80}B_{20}$ to be 2·46 and 2·55 without and with the use of an asymmetry parameter. Using a suitable reference material (crystalline Ni_2B) Wong and Liebermann (1984), on the other hand, have estimated bond distances ranging from 2·11 to 2·46 for the first three shells in $Ni_{66}B_{33}$ glass. The problem of EXAFS data analysis in metallic glasses is thus yet to be finally resolved. Within these constraints we would like to assert that the values of bond distances determined by us deserve adequate attention because of (a) their consistency and (b) our choice of suitable reference material in each case and their extreme sensitivity to the nature of bonding and degree of disorder as manifested by the dependence of the potential parameter $\bar{V}$ in XANES and that of constant α in EXAFS.

Acknowledgements

One of us (KBG) thanks the Royal Society and the SERC (UK) and the DST (India) for financial support. Thanks are also due to G Diakun and D Norman for valuable assistance.

References

Agarwal B K and Verma L P 1970 *J. Phys.* **C3** 535
Bianconi A, Dell'Ariccia M, Gargano A and Natoli C R 1983 *EXAFS and near edge structure* (eds) A Bianconi, L Incoccia and S Stipcich (Berlin: Springer-Verlag) p. 57
Cargrill III G S 1984, *J. Non-Cryst Solids* **61/62** 261
Chen H S, Fujiwara T and Waseda Y 1982 *J. Mater. Sci.* **17** 1337
Crescenzi M De, Balzarotti A, Comin F, Incoccia L, Mobilio S and Bacci D 1980 *J. Phys. Colloq.* **C8** 238
Crescenzi M De, Balzarotti A, Comin F, Incoccia L, Mobilio S and Motta N 1981 *Solid State Commun.* **37** 921
Defrain A, Bosio L, Cortes R and Da Costa P G 1984 *J. Non-Cryst. Solids* **61/62** 439
Dubois J M and Caer G Le 1982 *J. Phys. (Paris)* 43 **C9** 67
Durham P J 1983 *EXAFS and near edge structure* (eds) A Bianconi, L Incoccia and S Stipcich (Berlin: Springer-Verlag) p. 37
Eisenberger P and Brown G S 1979 *Solid State Commun.* **29** 481
Garg K B and Chauhan H S 1986 *J. Physics D* (communicated)
Gaskell P H, Glover D M, Livesey A K, Durham P J and Greaves G N 1982 *J. Phys.* **C15** 597
Goulon J, Goulon-Ginet C, Cortes R and Dubois J M 1982 *J. Phys.* **43** 539
Gurnam S J, Ginsted N and Ross I 1984 *J. Phys.* **C17** 143
Haensel R, Rabe P, Tolkeihn G and Weener A 1980 *Proc. NATO Adv. Inst: Liquid and amorphous metals* p. 459
Hayes T M, Allen J W, Tauc J, Giessen B C and Hausen J J 1978 *Phys. Rev. Lett.* **40** 1282
Lamparter P, Sperl W, Steeb S and Bletry J 1982 *Z. Naturforsch* **A37** 1223
Lokhande N R and Chetal A R 1978 *J. Phys. Soc. Jpn* **45** 212
Lytle F W, Sayers D E and Stern 1975 *Phys. Rev.* **B11** 4825
Nold E, Lamparter P, Olbrich H, Rainer-Harbach G and Steeb S 1981 *Z. Naturforsch* **A36** 1932
Norman D, Garg K B and Durham P J 1985 *Solid State Commun.* **56** 895
Paasche F, Olbrich H, Rainer-Harbach G, Lamparter P.and Steeb S 1982 *Z. Naturforsch* **A37** 1215
Polk D E 1970 *Scr. Metall.* **4** 117
Raoux D, Flank A M and Sadoc A 1983 *EXAFS and Near edge structure* (eds) A Bianconi, L Incoccia and S Stipcich (Berlin: Springer Verlag) p. 232
Sayers D E, Lytle F W and Stern E A 1970 *Adv. X-ray Anal.* **13** 248
Szmulowicz F and Pease D M 1978 *Phys. Rev.* **B17** 3341
Wong J 1981 *Topics of applied physics* (eds) H J Güdtherodt and H Beck (New York: Springer) Vol. 46 p. 45
Wong J and Liebermann H H 1984 *Phys. Rev.* **B29** 651